DTIC COPY

REPORT DOCUMENTATION PAGE

Form Approved
OMB No. 0704-01-0188

PLEASE DO NOT RETURN YOUR FORM TO THE ABOVE ADDRESS.

1. REPORT DATE *(DD-MM-YYYY)*	2. REPORT TYPE	3. DATES COVERED *(From - To)*
20-02-2009	REPRINT	

4. TITLE AND SUBTITLE

Numerical modeling of multidimensional diffusion in the radiation belts using layer methods

5a. CONTRACT NUMBER

5b. GRANT NUMBER

5c. PROGRAM ELEMENT NUMBER
621010F

6. AUTHORS
Xin Tao*
Jay M. Albert
Anthony A. Chan*

5d. PROJECT NUMBER
1010

5e. TASK NUMBER
RS

5f. WORK UNIT NUMBER
A1

7. PERFORMING ORGANIZATION NAME(S) AND ADDRESS(ES)

Air Force Research Laboratory /RVBXR
29 Randolph Road
Hanscom AFB, MA 01731-3010

8. PERFORMING ORGANIZATION REPORT NUMBER
AFRL-RV-HA-TR-2011-1016

9. SPONSORING/MONITORING AGENCY NAME(S) AND ADDRESS(ES)

10. SPONSOR/MONITOR'S ACRONYM(S)
AFRL/RVBXR

11. SPONSOR/MONITOR'S REPORT NUMBER(S)

12. DISTRIBUTION/AVAILABILITY STATEMENT
Approved for Public Release; distribution unlimited.

13. SUPPLEMENTARY NOTES
Reprinted from *Journal of Geophysical Research*, Vol. 114, A02215, doi:10.1029/2008JA013826, 2009
*Department of Physics and Astronomy, Rice University, Houston, TX

14. ABSTRACT

A new code using layer methods is presented to solve radiation belt diffusion equations and is used to explore effects of cross diffusion on electron fluxes. Previous results indicate that numerical problems arise when solving diffusion equations with cross diffusion when using simple finite difference methods. We show that layer methods, which are based on stochastic differential equations, are capable of solving diffusion equations with cross diffusion and are also generalizable to three dimensions. We run our layer code using two chorus wave models and a combined magnetosonic wave and hiss wave model (MH wave model). Both chorus and magnetosonic waves are capable of accelerating electrons to MeV levels in about a day. However, for the chorus wave models, omitting cross diffusion overestimates fluxes at high energies and small pitch angles, while for the MH wave model, ignoring cross diffusion overestimates fluxes at high energies and large pitch angles. These results show that cross diffusion is not ignorable and should be included when calculating radiation belt fluxes.

15. SUBJECT TERMS

Radiation belt | Cross diffusion | Electron flux | Chorus wave | Magnetosonic wave

16. SECURITY CLASSIFICATION OF:			17. LIMITATION OF ABSTRACT	18. NUMBER OF PAGES	19a. NAME OF RESPONSIBLE PERSON
a. REPORT	b. ABSTRACT	c. THIS PAGE			James I. Metcalf
UNCL	UNCL	UNCL	UNL	10	19B. TELEPHONE NUMBER *(Include area code)*

JOURNAL OF GEOPHYSICAL RESEARCH, VOL. 114, A02215, doi:10.1029/2008JA013826, 2009

Numerical modeling of multidimensional diffusion in the radiation belts using layer methods

Xin Tao,[1] Jay M. Albert,[2] and Anthony A. Chan[1]

Received 15 October 2008; revised 26 November 2008; accepted 17 December 2008; published 20 February 2009.

[1] A new code using layer methods is presented to solve radiation belt diffusion equations and is used to explore effects of cross diffusion on electron fluxes. Previous results indicate that numerical problems arise when solving diffusion equations with cross diffusion when using simple finite difference methods. We show that layer methods, which are based on stochastic differential equations, are capable of solving diffusion equations with cross diffusion and are also generalizable to three dimensions. We run our layer code using two chorus wave models and a combined magnetosonic wave and hiss wave model (MH wave model). Both chorus and magnetosonic waves are capable of accelerating electrons to MeV levels in about a day. However, for the chorus wave models, omitting cross diffusion overestimates fluxes at high energies and small pitch angles, while for the MH wave model, ignoring cross diffusion overestimates fluxes at high energies and large pitch angles. These results show that cross diffusion is not ignorable and should be included when calculating radiation belt electron fluxes.

Citation: Tao, X., J. M. Albert, and A. A. Chan (2009), Numerical modeling of multidimensional diffusion in the radiation belts using layer methods, *J. Geophys. Res.*, *114*, A02215, doi:10.1029/2008JA013826.

1. Introduction

[2] The Earth's outer radiation belt is very dynamic, and electron fluxes can vary by several orders of magnitude during storm times, which makes it very hazardous to spacecraft and astronauts [e.g., *Baker et al.*, 1986, 1994, 1997]. Quasi-linear diffusion theory has been used to evaluate dynamic changes of particle fluxes in the radiation belts [*Albert*, 2004; *Albert and Young*, 2005; *Horne and Thorne*, 2003; *Horne et al.*, 2003; *Li et al.*, 2007; *Varotsou et al.*, 2005]. *Albert* [2004] and *Albert and Young* [2005] show that numerical problems arise when solving multidimensional quasi-linear diffusion equations using standard finite difference methods, because of rapidly varying off-diagonal terms. Thus different numerical techniques have been employed to solve multidimensional diffusion equations, e.g., *Albert and Young* [2005] and *Tao et al.* [2008] (henceforth denoted as paper 1).

[3] In paper 1, we developed a stochastic differential equation (SDE) code to solve 2-D bounce-averaged pitch angle and energy diffusion equations. The SDE code is very efficient when solutions on a small number of points are needed. However, if solutions are needed on a large computational domain for long times, the SDE code becomes less efficient, for reasons explained in paper 1. *Milstein* [2002], *Milstein and Tretyakov* [2002] and *Milstein and Tretyakov* [2001] have used properties of numerical integration of SDEs to develop so-called layer methods, which are deterministic, to solve parabolic equations successively in time. In this paper we develop a code using layer methods and show that it is able to solve 2-D radiation belt diffusion equations with cross diffusion and it is generalizable to three dimensions. Although the layer code does not have the high parallelization efficiency compared with the SDE code in paper 1, it is more efficient when solving the diffusion equation over a large computational domain for long times. Also our layer code can handle boundary conditions with complicated geometry rather than coordinate-equal-constant type boundaries that are typically used in standard finite difference codes.

[4] Using this layer code, we then explore effects of ignoring off-diagonal terms when modeling wave-particle interactions in the radiation belts. Previous works show that chorus waves and magnetosonic waves are observed during storm times and are possible candidates of accelerating electrons to MeV on a time scale of days [e.g., *Horne and Thorne*, 1998; *Horne et al.*, 2005, 2007; *Meredith et al.*, 2008]. Superluminous (RX, LO, LX mode) waves have also been shown to be possible candidates of energizing electrons [*Xiao et al.*, 2006] if they are present under appropriate conditions [*Xiao et al.*, 2007], but there have been no direct observations of these waves in the radiation belts so far. On the other hand, interactions with EMIC waves, chorus waves and hiss waves have been invoked as important loss mechanisms of radiation belt electrons [e.g., *Lyons and Thorne*, 1973; *Summers and Thorne*, 2003; *Li et al.*, 2007]. In this work, we use two wave models: the chorus wave model from *Li et al.* [2007], and the combined magnetosonic wave [*Horne et al.*, 2007] and hiss wave [*Li et al.*, 2007] (MH) model. In paper 1, we showed that ignoring off-diagonal terms causes errors of an order of magnitude for 2 MeV electrons at small pitch angles using the *Horne et al.* [2005] chorus wave model. Using the *Li et al.*

[1]Department of Physics and Astronomy, Rice University, Houston, Texas, USA.
[2]Air Force Research Laboratory, Space Vehicles Directorate, Hanscom Air Force Base, Massachusetts, USA.

0148-0227/09/2008JA013826$09.00

[2007] chorus wave model and the MH wave model is helpful in understanding the sensitivity of the main conclusions of paper 1 to different wave models.

[5] The remainder of this paper is organized as follows. We introduce the layer methods by using a simple initial-value problem in section 2. Details of our 2-D layer code to solve a bounce-averaged pitch angle and energy diffusion equation are given in section 3. We first show its agreement with *Albert and Young* [2005] results in section 3.1. Then we solve the diffusion equation with diffusion coefficients calculated using the *Li et al.* [2007] chorus wave model (section 3.2) and the MH wave model (section 3.3) to show effects of ignoring off-diagonal terms and energization of electrons. Our results are then discussed and summarized in section 4.

2. Milstein Layer Methods

[6] In this section, we will use an initial-value problem to illustrate the layer methods shown in *Milstein* [2002]. Boundary conditions can be implemented in a similar way as described by paper 1, or by *Milstein and Tretyakov* [2001] and *Milstein and Tretyakov* [2002].

2.1. One-Step Representation of Solutions Using the SDE Method

[7] Assume that we want to solve the equation

$$\frac{\partial f}{\partial t} = \sum_{i=1}^{d} b_i(t,\boldsymbol{x})\frac{\partial f}{\partial x_i}(t,\boldsymbol{x}), + \sum_{i,j=1}^{d}\frac{1}{2}a_{ij}(t,\boldsymbol{x})\frac{\partial^2 f}{\partial x_i x_j}(t,\boldsymbol{x}) \tag{1}$$

with initial condition $f(t_0, \boldsymbol{x}) = g(\boldsymbol{x})$. First, we discretize time t equidistantly to $t_0, \cdots, t_n, t_{n+1}, \cdots$, and assume that we know solutions of all f at time t_n, which means that now $f(t_n, \boldsymbol{x})$ can be considered as an initial condition when solving $f(t_{n+1}, \boldsymbol{x})$. Then using the SDE method described in paper 1, we have

$$f(t_{n+1},\boldsymbol{x}) \approx \mathbb{E}\ (f(t_n,\tilde{\boldsymbol{x}})), \tag{2}$$

where $\mathbb{E}$ is the expectation value and $\tilde{\boldsymbol{x}}$ is given by

$$\tilde{\boldsymbol{x}} = \boldsymbol{x} + b(t_{n+1},\boldsymbol{x})\Delta t + \sigma(t_{n+1},\boldsymbol{x})\Delta \boldsymbol{W}. \tag{3}$$

Here $\Delta t = t_{n+1} - t_n$, σ is related to $\boldsymbol{a}$ by $\sigma\sigma^T = \boldsymbol{a}$ and $\Delta \boldsymbol{W} \equiv (\Delta W_1, \Delta W_2, \ldots, \Delta W_d)$ is one increment of a Wiener random process [*Gardiner*, 1985].

[8] Numerically $\Delta \boldsymbol{W}$ can be generated from a vector of standard Gaussian random numbers with zero mean and unit variance, as we did in paper 1, or we can choose the probability distribution of the components to be

$$P\left(\Delta W_i = \pm\sqrt{\Delta t}\right) = \frac{1}{2}, \quad i = 1, 2, \cdots, d, \tag{4}$$

where P denotes the probability [*Milstein*, 2002]. Substituting ΔW_i from equation (4) into equation (3), we will have 2^d possible $\Delta \boldsymbol{W}$'s, thus 2^d possible $\tilde{\boldsymbol{x}}$'s, each with probability $1/2^d$. The expectation value term in equation (2) can then be rewritten as

$$f(t_{n+1},\boldsymbol{x}) \approx \mathbb{E}\ (f(t_n,\tilde{\boldsymbol{x}})) = \frac{1}{2^d}\sum_{j=1}^{2^d} f(t_n,\tilde{\boldsymbol{x}}_j). \tag{5}$$

[9] Note that in reality, we usually do not know f at t_n and at an arbitrary point $\tilde{x}_j$. This is why we trace trajectories back to the initial condition in paper 1. However, as described by *Milstein* [2002], we can use interpolations to obtain $f(t_n, \tilde{x}_j)$ from already known f's at fixed grid points to make a convergent algorithm. In this way, we obtain solutions successively from time layer t_n to t_{n+1}, hence the name "layer methods" [*Milstein*, 2002].

2.2. A Simple Layer Method Algorithm

[10] A simple interpolation method is linear interpolation. Take a 1-D diffusion equation for example:

$$\frac{\partial f}{\partial t} = b\frac{\partial f}{\partial x} + \frac{1}{2}\sigma^2\frac{\partial^2 f}{\partial x^2}. \tag{6}$$

First, discretizing $\boldsymbol{x}$ equidistantly into $x_0, x_1, x_2, \cdots, x_N$, we have

$$f(t_n,\tilde{x}) = \frac{x_{i+1}-\tilde{x}}{x_{i+1}-x_i}f(t_n,x_i) + \frac{\tilde{x}-x_i}{x_{i+1}-x_i}f(t_n,x_{i+1}) + \mathcal{O}(\Delta x^2), \qquad x_i \le \tilde{x} \le x_{i+1}, \tag{7}$$

where x_i and x_{i+1} are fixed grid points, and $\Delta x \equiv x_{i+1} - x_i$. Then a simple layer method algorithm for a 1-D diffusion problem is

$$f(t_{n+1},x_j) = \frac{1}{2}[f(t_n,\tilde{x}_1) + f(t_n,\tilde{x}_2)], \qquad j = 1, 2, \ldots, N-1, \tag{8}$$

$$\tilde{x}_1 = x_j + b\Delta t + \sigma\sqrt{\Delta t}, \tag{9}$$

$$\tilde{x}_2 = x_j + b\Delta t - \sigma\sqrt{\Delta t}, \tag{10}$$

$$f(t_0,x_j) = g(t_0,x_j), \tag{11}$$

with $f(t_n, \tilde{x}_{1,2})$ calculated using equation (7). We see from equations (7) to (11) that negative values of f cannot arise from this procedure. A proof that the one-step error of the above algorithm is $\mathcal{O}(\Delta t^2)$ is given in Appendix A. Also we show the connection between layer methods with bilinear interpolation and conventional finite difference methods in Appendix B for a simple 2-D diffusion equation without cross diffusion.

[11] Dirichlet and Neumann boundary conditions can be implemented in a similar way as described in paper 1. For example, if we have a Dirichlet boundary $f(t, x_0) = g_0(t, x_0)$, we replace $\tilde{x}$ by x_0 if $\tilde{x} < x_0$; if we have a Neumann boundary $\partial f/\partial x\ (t, x_N) = 0$, then we replace $\tilde{x}$ by $2x_N - \tilde{x}$ if $\tilde{x} > x_N$. For more general ways of handling boundary conditions, we refer readers to *Milstein and Tretyakov* [2001, 2002].

3. Application

[12] In this section, we apply the layer method described in section 2 to the bounced-averaged equatorial pitch angle

(α_0) and momentum (p) diffusion equation in the radiation belts

$$\frac{\partial f}{\partial t} = \frac{1}{Gp}\frac{\partial}{\partial \alpha_0} G\left(D_{\alpha_0\alpha_0}\frac{1}{p}\frac{\partial f}{\partial \alpha_0} + D_{\alpha_0 p}\frac{\partial f}{\partial p}\right) + \frac{1}{G}\frac{\partial}{\partial p} G\left(D_{\alpha_0 p}\frac{1}{p}\frac{\partial f}{\partial \alpha_0} + D_{pp}\frac{\partial f}{\partial p}\right), \quad (12)$$

where $D_{\alpha 0\alpha 0}$, $D_{\alpha 0 p}$ and D_{pp} are bounce-averaged pitch angle, mixed and momentum diffusion coefficients [*Albert*, 2004]. Here G is a Jacobian factor, $G = p^2 T(\alpha_0)\sin(\alpha_0)\cos(\alpha_0)$, and $T(\alpha_0) \approx 1.30 - 0.56\sin(\alpha_0)$ is the normalized bounce period. Initial and boundary conditions are chosen to be the same as those of *Albert and Young* [2005] and paper 1. Thus the initial flux is

$$j(t = 0) = \exp[-(E - 0.2)/0.1][\sin(\alpha_0) - \sin(\alpha_{0L})], \quad (13)$$

where the loss cone angle $\alpha_{0L} = 5°$ and flux j is related to phase-space density f by $j = f/p^2$. Boundary conditions are

$$f|_{\alpha_0 = \alpha_{0L}} = 0, \quad (14)$$

$$\left.\frac{\partial f}{\partial \alpha_0}\right|_{\alpha_0 = 90°} = 0, \quad (15)$$

$$f|_{E = E_{max}} = 0, \quad (16)$$

$$f|_{E = E_{min}} = j(t = 0)|_{E = E_{min}}/p_{min}^2 \quad (17)$$

where $E_{min} = 0.2$ MeV and $E_{max} = 5$ MeV, and p_{min} is the momentum corresponding to E_{min} [*Albert and Young*, 2005].

[13] We write a code using the layer method to solve the diffusion equation (12). Discretize α_0 and $y \equiv \log E$ equidistantly into $N_{\alpha 0}$ and N_y grid cells, and thus $\Delta\alpha_0 = (\pi/2 - \alpha_{0L})/N_{\alpha 0}$ and $\Delta y = (y_{max} - y_{min})/N_y$. The equation we use to solve f is

$$f(t_{n+1}, \alpha_{0i}, y_j) = \frac{1}{4}\sum f\left[t_n, \tilde{\alpha}_{0i}(\Delta W_1, \Delta W_2), \tilde{y}_j(\Delta W_1, \Delta W_2)\right], \quad (18)$$

where

$$\tilde{\alpha}_{0i} = \alpha_{0i} + b_{\alpha_0}\Delta t + \sigma_{11}\Delta W_1 + \sigma_{12}\Delta W_2, \quad (19)$$

$$\tilde{p}_j = p_j + b_p\Delta t + \sigma_{21}\Delta W_1 + \sigma_{22}\Delta W_2, \quad (20)$$

and $\tilde{y}_j$ is then obtained from $\tilde{p}_j$. If $\tilde{\alpha}_{0i} < \alpha_{0L}$ or $\tilde{\alpha}_{0i} > \pi/2$, we replace $\tilde{\alpha}_{0i}$ by α_{0L} or $\pi - \tilde{\alpha}_{0i}$, respectively. If $\tilde{p} < p_{min}$ or $\tilde{p} > p_{max}$, we set $\tilde{p} = p_{min}$ or $\tilde{p} = p_{max}$, respectively. In equations (18) to (20), ΔW_1 and ΔW_2 each takes value $\pm\sqrt{\Delta t}$, and the summation in equation (18) sums over four different combinations of (ΔW_1, ΔW_2). The functions b and σ are the same as in paper 1:

$$b_{\alpha_0} = \frac{1}{Gp}\frac{\partial}{\partial \alpha_0}\left(\frac{GD_{\alpha_0\alpha_0}}{p}\right) + \frac{1}{G}\frac{\partial}{\partial p}\left(\frac{GD_{\alpha_0 p}}{p}\right), \quad (21)$$

$$b_p = \frac{1}{Gp}\frac{\partial}{\partial \alpha_0}(GD_{\alpha_0 p}) + \frac{1}{G}\frac{\partial}{\partial p}(GD_{pp}), \quad (22)$$

$$\sigma_{11} = \sqrt{2D_{\alpha_0\alpha_0}}/p, \quad (23)$$

$$\sigma_{12} = 0, \quad (24)$$

$$\sigma_{21} = \sqrt{2}D_{\alpha_0 p}/\sqrt{D_{\alpha_0\alpha_0}}, \quad (25)$$

$$\sigma_{22} = \sqrt{2D_{pp} - \sigma_{21}^2}. \quad (26)$$

With the choice of bilinear interpolation to obtain $f(t_n, \tilde{\alpha}_{0i}, \tilde{y}_j)$ in equation (18) from its neighboring grid points, the above algorithm has a global error of $O(\Delta t)$ when $\Delta\alpha = c_\alpha\Delta t$, $\Delta y = c_y\Delta t$, where c_α and c_y are two constants [*Milstein*, 2002]. *Milstein* [2002] suggests without proof that it may be possible to use cubic interpolation to obtain a higher convergence rate. We conducted numerical experiments using cubic interpolation and found that this does not guarantee positive values. Probably a more sophisticated method would give both high accuracy and positivity, but we chose to use bilinear interpolation in our code for simplicity.

3.1. Comparison With *Albert and Young* [2005] Results

[14] To show that layer methods can be used to solve the diffusion equation (12), we compare results calculated using our layer code with results of *Albert and Young* [2005] using the same diffusion coefficients. The diffusion coefficients are calculated using the *Horne et al.* [2005] storm time chorus wave model at $L = 4.5$. Wave parameters are shown in Table 1 for a comparison with the *Li et al.* [2007] storm time chorus wave model (see section 3.2).

[15] We choose $\Delta t = 4 \times 10^{-4}$ day to give a relatively small change of $\Delta\alpha_0$ and Δy, compared with the computational domain. We plot fluxes of 0.5 MeV and 2 MeV at $t = 2$ d in Figure 1 to show the convergence of solutions with respect to $N_{\alpha 0}$ and N_y, and this leads to our choice of $N_{\alpha 0} = 1400$ and $N_y = 1500$. Comparisons with results from *Albert and Young* [2005] are shown in Figure 2 for $E = 0.5$ MeV (top) and $E = 2$ MeV (bottom) electrons. Considering the small errors associated with each method, we conclude that the two sets of results agree very well with each other and our layer code is capable of solving the bounce-averaged pitch angle and momentum diffusion equation (12) with cross diffusion. In the next section, we apply our layer code to the diffusion equation with diffusion coefficients calculated using the *Li et al.* [2007] chorus wave model.

Table 1. Local Time Sector Distribution, Latitudinal Distribution $|\lambda|$ of the Waves, Equatorial Ratio of Electron Plasma to Gyro Frequencies f_{pe}/f_{ce}, and Wave Magnetic Field Amplitude of Wave Models B_w From *Horne et al.* [2005] and *Li et al.* [2007]

	Horne et al. [2005]			*Li et al.* [2007]	
	2300–0600 MLT	0600–1200 MLT	1200–1500 MLT	0000–0600 MLT	0600–1200 MLT
$\|\lambda\|$	0 to 15°	15° to 35°	10° to 35°	0° to 15°	0° to 35°
f_{pe}/f_{ce}	3.43	4.0	6.72	3.8	4.6
B_w	50 pT	100 pT	50 pT	50 pT	$10^{0.75+0.04\lambda}$ pT

3.2. Effects of Ignoring Cross Diffusion in *Li et al.* [2007] Chorus Wave Model

[16] *Li et al.* [2007] used a new chorus wave model and calculated changes of electron fluxes due to cyclotron resonances with chorus waves by solving a 2-D bounce-averaged pitch angle and energy diffusion equation using an implicit numerical scheme. However, cross diffusion is not included in their calculation [*Li et al.*, 2007]. In this work, we calculate diffusion coefficients including cross diffusion using the *Li et al.* [2007] main phase storm time chorus wave model. We also use a wave normal angle distribution from *Horne et al.* [2005], in contrast to *Li et al.* [2007], who use a parallel propagation approximation. The resulting diffusion coefficients are shown in Figure 3. By solving the diffusion equation with off-diagonal terms using our layer code, we show in this section effects of ignoring off-diagonal terms on electron fluxes using the *Li et al.* [2007] chorus wave model.

[17] For comparison with conclusions in paper 1, the boundary and initial conditions are the same as equations (13)–(17), thus they are different from those in *Li et al.* [2007]. Figure 4 shows color plots of fluxes calculated using the diffusion coefficients from *Li et al.* [2007] chorus waves at t = 0.1, 1 and 2 days. Both results with (plots on left) and without (plots on right) cross diffusion are shown for comparison. We see from Figure 4 that at high energies ignoring cross diffusion overestimates fluxes at lower pitch angles and creates a peak in fluxes around 20°. This can be seen more clearly from Figure 5, which shows line plots of fluxes calculated with and without cross diffusion at t = 0.1, 1 and 2 days for 0.5 MeV and 2 MeV electrons. At t = 0.1 day, the error caused by ignoring cross diffusion is small for 0.5 MeV electrons at all pitch angles and 2 MeV electrons at high pitch

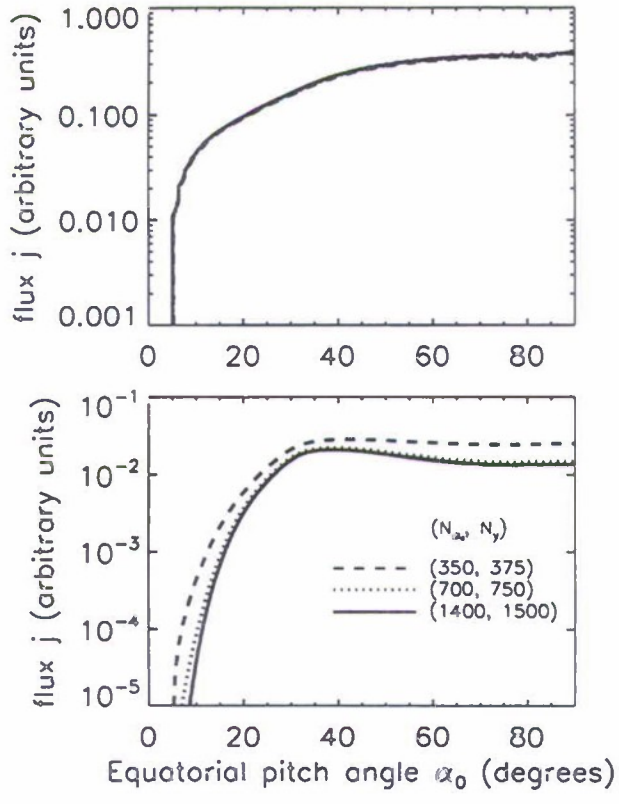

Figure 1. Fluxes for (top) E = 0.5 MeV and (bottom) E = 2.0 MeV at t = 2 d with different choices of $N_{\alpha 0}$ and N_v using *Horne et al.* [2005] chorus wave model. In the top plot the three lines are very close together, in contrast to the larger separations shown in the bottom plot.

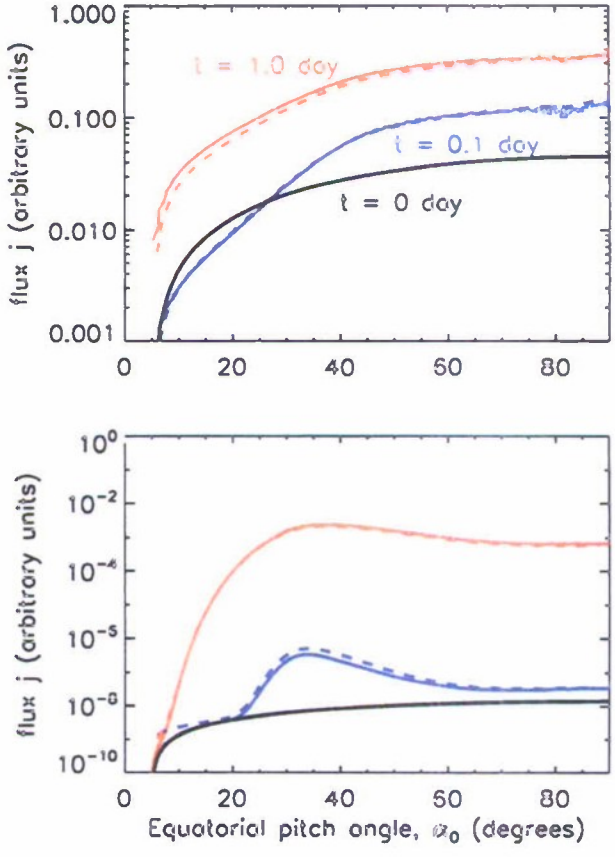

Figure 2. Comparisons between results obtained from the layer method (solid lines) and the *Albert and Young* [2005] method (dashed lines) for (top) E = 0.5 MeV and (bottom) E = 2.0 MeV at t = 0.1 day (blue lines) and t = 1.0 day (red lines). Here black lines show the initial condition.

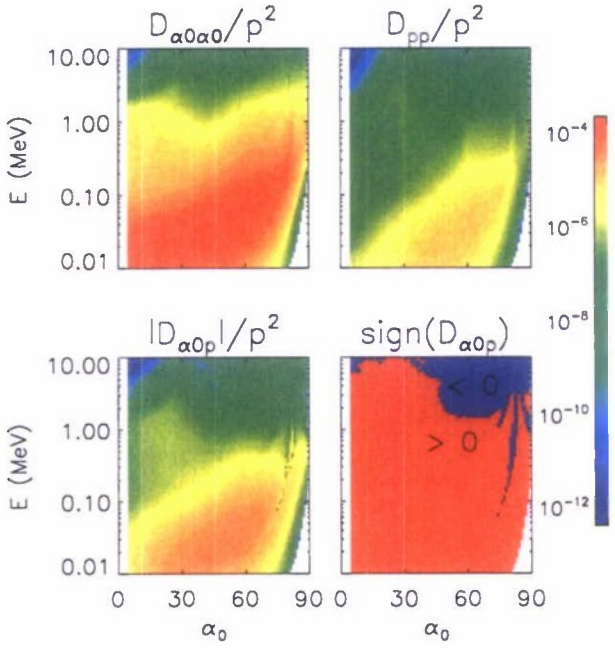

Figure 3. Inverse time scales in units of s^{-1} from diffusion coefficients calculated using *Li et al.* [2007] chorus wave model with the wave normal angle distribution from *Horne et al.* [2005]. The last plot shows the sign of the cross diffusion coefficients.

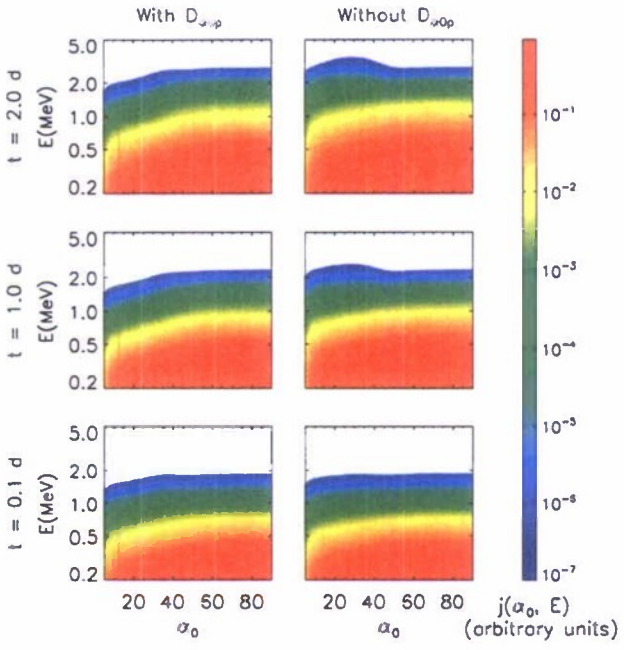

Figure 4. Fluxes calculated by the layer code using *Li et al.* [2007] chorus wave model at $t = 0.1$, 1, and 2 days. The plots on the left show fluxes with cross diffusion, and the plots on the right show fluxes without cross diffusion.

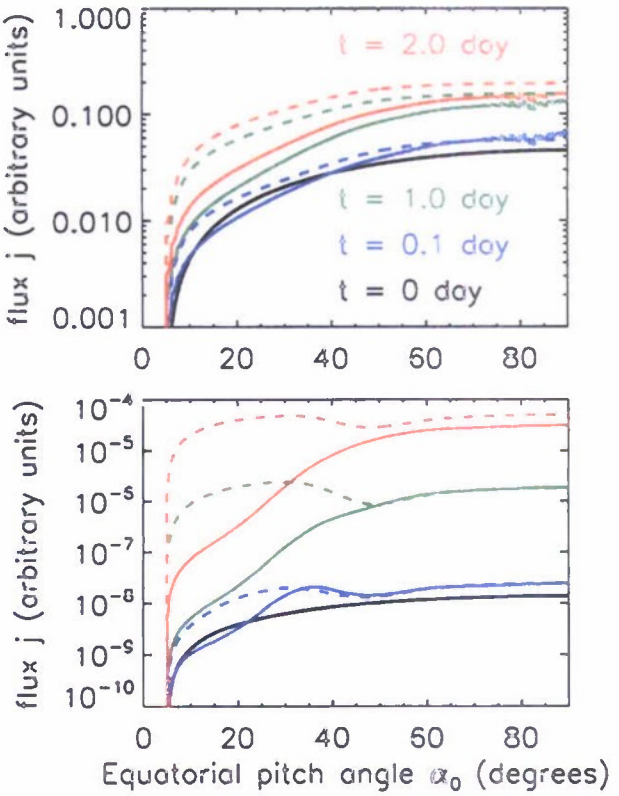

Figure 5. Fluxes for (top) $E = 0.5$ MeV and (bottom) $E = 2.0$ MeV at $t = 0.1$ day (blue lines), $t = 1$ day (green lines), and $t = 2.0$ day (red lines) with and without off-diagonal diffusion terms, calculated using *Li et al.* [2007] chorus wave model. Black lines show the initial condition. Dashed lines are results without off-diagonal diffusion coefficients, and solid lines are results with off-diagonal terms.

angles. For 2 MeV electrons at low pitch angles, however, the error is about a factor of ~10. At $t = 1$ and 2 days, at 0.5 MeV, ignoring cross diffusion overestimates fluxes at small pitch angles by only a factor of $2 \sim 3$. However, at 2 MeV, ignoring cross diffusion causes an error of about two orders of magnitude at small pitch angles. Thus, similar to results in paper 1, ignoring off-diagonal terms has a relatively small effect on fluxes for lower-energy electrons at higher pitch angles, but it introduces larger errors for larger energy electrons at lower pitch angles.

[18] To understand the similarity between conclusions obtained here and in paper 1, we now discuss features of the *Li et al.* [2007] and *Horne et al.* [2005] wave models, whose parameters are listed in Table 1. First, both *Li et al.* [2007] and *Horne et al.* [2005] wave models have similar latitudinal cutoffs of chorus wave power. For *Li et al.* [2007]: $|\lambda| < 35°$ on the dayside, and $|\lambda| < 15°$ on the nightside, for *Horne et al.* [2005]: $15° < |\lambda| < 35°$ in the prenoon sector, $10° < |\lambda| < 35°$ for the afternoon sector, and $|\lambda| < 15°$ on the nightside. We see larger errors at smaller pitch angles with both models. Second, even though the *Li et al.* [2007] chorus wave model has a dayside wave power increasing with latitude, which gives a more abrupt cutoff at the maximum latitude than the *Horne et al.* [2005] wave model, the actual values of the wave

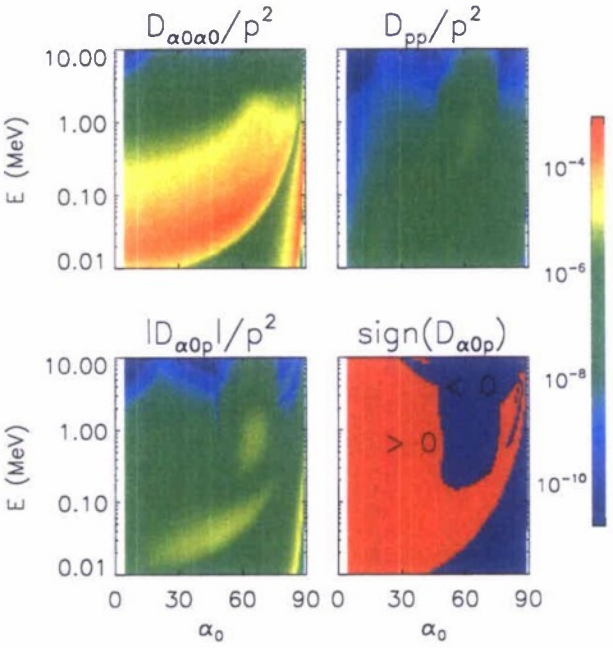

Figure 6. Inverse time scales in units of s^{-1} from diffusion coefficients calculated using a combined magnetosonic wave [*Horne et al.*, 2007] and hiss wave [*Li et al.*, 2007] model. The last plot shows the sign of the cross diffusion coefficients.

amplitude are not very different. At $\lambda = 0°$, the drift-averaged wave amplitude for the *Li et al.* [2007] wave model is 6/24 × 5.6 pT + 6/24 × 50 pT = 13.9 pT, while the *Horne et al.* [2005] model gives 7/24 × 50 pT = 14.6 pT. At $\lambda = 35°$, the drift-averaged wave amplitude for the *Li et al.* [2007] model in main phase is 6/24 × 141.25 pT + 6/24 × 50 pT = 47.8 pT, while the *Horne et al.* [2005] model gives 6/24 × 100 pT + 3/24 × 50 pT = 31.25 pT. Thus we see that both models assume zero amplitude above 35° latitude and have comparable wave power levels, so it is not too surprising to see similar conclusions on ignoring cross diffusion from the two wave models.

3.3. Evolution of Electron Fluxes Using a Model of Fast Magnetosonic Waves and Hiss

[19] Interactions with fast magnetosonic waves have been recently suggested by *Horne et al.* [2007] to be a possible important acceleration mechanism. Because these interactions typically only involve the Landau resonance ($n = 0$), coupling of diffusion in α_0 and p is expected to be especially important for them. For the wave model given by *Horne et al.* [2007], the quasi-linear diffusion coefficients of the magnetosonic waves are nonzero only over a limited range of pitch angle and energy [see *Albert*, 2008, Figure 9]. Thus we combine the magnetosonic wave model of *Horne et al.* [2007] outside the plasmasphere with the main phase hiss wave model in plumes from *Li et al.* [2007].

[20] The MLT averaged diffusion coefficients from magnetosonic waves (60%) and hiss waves (15%) are shown in Figure 6. A similar numerical experiment as Figure 1 is used to determine that $N_{\alpha 0} = 1400$ and $N_y = 1500$ is necessary to obtain accurate solutions. The resulting evolution of electron fluxes are plotted in Figure 7 at $t = 0.1$, 1 and 2 day. We see from the plots on the left (results with $D_{\alpha 0 p}$) that the magnetosonic waves can accelerate electrons to MeV on time scales of a day, and the fluxes show a peak around 55°, producing a butterfly distribution, at high energies. Comparing the plots on the left with the plots on the right (results without $D_{\alpha 0 p}$), we see that ignoring cross diffusion overestimates fluxes at larger energies and larger pitch angles (>55°), which is different from the effects using the *Horne et al.* [2005] and *Li et al.* [2007] chorus wave models. The effects of ignoring cross diffusion can be seen more clearly in Figure 8, which shows fluxes versus equatorial pitch angle at $t = 0.1$, 1 and 2 days for 0.5 and 2 MeV. We see that for 0.5 MeV electrons, effects of ignoring cross diffusion are small at all pitch angles. However, for 2 MeV electrons, ignoring cross diffusion overestimates fluxes at large pitch angles (>55°) by a factor of 5 ~ 10 at all three times, and by a factor of ~5 at small pitch angles at $t = 1$ and 2 days.

4. Summary and Discussion

[21] In this work, we introduce the layer method, which is based on the SDE method of paper 1, to solve multidimensional radiation belt diffusion equations. Compared with the SDE method, the layer method is deterministic and more efficient when solutions on a large computational domain are needed for long times. Compared with finite difference methods, the layer methods are less efficient, but generalize to three dimensions easily and are able to handle complicated boundary geometries. We apply the layer method to a bounce-averaged pitch angle and energy diffusion equation and obtain excellent agreement with a previous method [*Albert and Young*, 2005] using the *Horne et al.* [2005] chorus wave

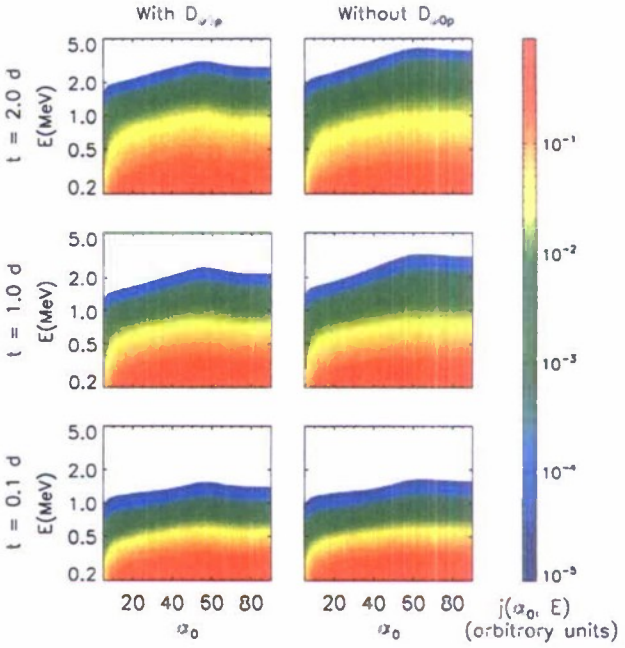

Figure 7. Fluxes calculated by the layer code using the MH wave model at $t = 0.1$, 1, and 2 days. The plots on the left show fluxes with cross diffusion, and the plots on the right show fluxes without cross diffusion.

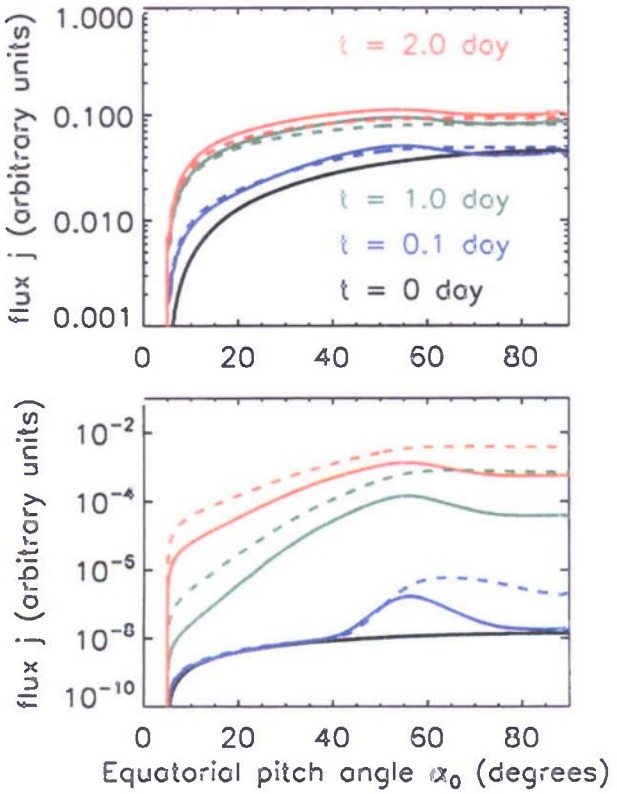

Figure 8. Fluxes for (top) $E = 0.5$ MeV and (bottom) $E = 2.0$ MeV at $t = 0.1$ day (blue lines), $t = 1$ day (green lines), and $t = 2.0$ day (red lines) with and without off-diagonal diffusion terms, calculated using the MH wave model. Black lines show the initial conditions. Dashed lines are results without off-diagonal diffusion coefficients, and solid lines are results with off-diagonal terms.

model. We show that our layer code is able to solve multi-dimensional diffusion equations with cross terms.

[22] We then use the layer code to evaluate effects of ignoring cross diffusion using the *Li et al.* [2007] chorus wave model, as a comparison with the *Horne et al.* [2005] chorus wave model used in paper 1. The main conclusion is similar to paper 1; that is, ignoring off-diagonal terms produces larger errors at smaller pitch angles and higher energies. We show in section 3.2 that this similarity might be due to the fact that both wave models have a latitudinal cutoff at 35° and comparable wave power levels.

[23] In section 3.3, we show evolution of electron fluxes using a combined magnetosonic wave [*Horne et al.*, 2005] and hiss wave model [*Li et al.*, 2007]. We show that, despite pitch angle scattering by hiss waves, electrons are energized to MeV in 2 days of simulation. Ignoring cross diffusion overestimates fluxes at larger pitch angles and higher energies, in contrast to the effects of ignoring cross diffusion using the *Horne et al.* [2005] and *Li et al.* [2007] chorus wave models. Overall, we conclude that cross diffusion terms are important and should be included when modeling diffusion of electrons in the outer radiation belt.

[24] With the layer method and other methods [*Tao et al.*, 2008; *Albert and Young*, 2005], it is now possible to simulate radiation belt diffusion with important cross diffusion included. However, to accurately model radiation belt dynamics, more accurate wave models and initial and boundary conditions should be used. For example, comparing Figures 4 and 7, it is easy to see that errors could be large if inaccurate wave models are used. Further work should be done with improved wave models as they become available. Also, effects of different initial conditions and boundary conditions, such as relativistic kappa-type functions [*Xiao et al.*, 2008], should be considered to improve radiation belt modeling.

Appendix A: One-Step Error of the Layer Method

[25] To calculate the one-step error of the layer method, consider a 1-D initial value problem,

$$\frac{\partial f}{\partial t} = b(t,x)\frac{\partial f}{\partial x} + \frac{1}{2}\sigma^2(t,x)\frac{\partial^2 f}{\partial x^2}, \qquad f(t_0,x) = g(x). \tag{A1}$$

With the layer method, we discretize t equidistantly into t_0, t_1, t_2, ... with time step h, and the approximate solution of equation (A1) at (t_{k+1}, x) is given by

$$f_{k+1}(x) = \frac{1}{2}f\left[t_k, x + b(t_{k+1},x) + \sigma(t_{k+1},x)\sqrt{h}\right] + \frac{1}{2}f\left[t_k, x + b(t_{k+1},x) - \sigma(t_{k+1},x)\sqrt{h}\right]. \tag{A2}$$

[26] To show the error of $f_{k+1}(x)$, we expand $f(t_{k+1} - h, x + b \pm \sigma\sqrt{h})$ using Taylor expansion and the resulting equation is

$$f\left(t_{k+1} - h, x + b \pm \sigma\sqrt{h}\right) = f(t_{k+1},x) - h\frac{\partial f}{\partial t} + \left(bh \pm \sigma\sqrt{h}\right)\frac{\partial f}{\partial x} + \frac{1}{2}\left(\sigma^2 h \pm 2b\sigma h^{\frac{3}{2}}\right)\frac{\partial^2 f}{\partial x^2} + \left(\mp\sigma h^{\frac{3}{2}}\right)\frac{\partial^2 f}{\partial t \partial x} + \left(\pm\sigma^3 h^{\frac{3}{2}}\right)\frac{1}{6}\frac{\partial^3 f}{\partial x^3} + O(h^2). \tag{A3}$$

Inserting equation (A3) into (A2) yields

$$f_{k+1}(x) = f(t_{k+1},x) - h\left(\frac{\partial f}{\partial t} - b\frac{\partial f}{\partial x} - \frac{1}{2}\sigma^2\frac{\partial^2 f}{\partial x^2}\right) + O(h^2). \tag{A4}$$

Using equation (A1), equation (A4) becomes

$$f_{k+1}(x) = f(t_{k+1},x) + O(h^2), \tag{A5}$$

which shows that the approximation $f_{k+1}(x)$ differs from the true solution $f(t_{k+1}, x)$ by a term proportional to h^2.

[27] In practice, we use interpolations to obtain $f(t_k, x + b \pm \sigma\sqrt{h})$ in equation (A2) from fixed grid points, denoted as $\bar{f}(t_k, x + b \pm \sigma\sqrt{h})$. For example, using linear interpolation, we have

$$\bar{f}\left(t_k, x + b \pm \sigma\sqrt{h}\right) = f\left(t_k, x + b \pm \sigma\sqrt{h}\right) + O(\Delta x^2). \tag{A6}$$

Thus with $\Delta x = c_x h$, where c_x is a constant, the error from interpolation is also $\mathcal{O}(h^2)$ and equation (A5) is not changed. Overall the one-step error of the above layer method is $\mathcal{O}(h^2)$. *Milstein* [2002] shows that the global error (the error accumulated from time t_0 to t) of the layer method is $\mathcal{O}(h)$.

Appendix B: Relationship Between Finite Difference Methods and Layer Methods

[28] Consider a 2-D diffusion equation with constant diffusion coefficients and no cross diffusion,

$$\frac{\partial f}{\partial t} = D_{xx}\frac{\partial^2 f}{\partial x^2} + D_{yy}\frac{\partial^2 f}{\partial y^2}. \tag{B1}$$

According to the layer method, the updated value of $f(x, y)$ after a time step Δt is just the average of f at the four points $f(x \pm L_x, y \pm L_y, t)$, where $L_x \equiv \sqrt{2D_{xx}\Delta t}$ and $L_y \equiv \sqrt{2D_{yy}\Delta t}$ according to the prescription in section 2.2. Use bilinear interpolation on a regular grid with spacing (Δx, Δy), and take Δt small enough that $L_x \le \Delta x$ and $L_y \le \Delta y$ so that the points $(x \pm L_x, y \pm L_y)$ lie within the neighboring grid cells.

[29] Then the value of f at grid point i, j and time t_{n+1}, f_{ij}^{n+1}, is given by

$$\begin{aligned} 4f_{ij}^{n+1} = {} & r_x r_y f_{i-1j+1}^n + 2(1-r_x) r_y f_{ij+1}^n + r_x r_y f_{i+1j+1}^n \\ & + 2r_x(1-r_y) f_{i-1j}^n + 4(1-r_x)(1-r_y) f_{ij}^n + 2r_x(1-r_y) f_{i+1j}^n \\ & + r_x r_y f_{i-1j-1}^n + 2(1-r_x) r_y f_{ij-1}^n + r_x r_y f_{i+1j-1}^n \end{aligned} \tag{B2}$$

where $r_x = L_x/\Delta x$ and $r_y = L_y/\Delta y$. Note that f_{ij}^{n+1} is guaranteed to be positive since all the coefficients of $f^n_{i\pm1j\pm1}$ are nonnegative.

[30] On the other hand, the conventional explicit finite difference scheme for equation (B1) can be written as

$$4f_{ij}^{n+1} = 2c_y f_{ij+1}^n + 2c_x f_{i-1j}^n + 4(1 - c_x - c_y) f_{ij}^n + 2c_x f_{i+1j}^n + 2c_y f_{ij-1}^n \tag{B3}$$

for time step Δt, where $c_x = 2D_{xx}\Delta t/(\Delta x)^2$ and $c_y = 2D_{yy}\Delta t/(\Delta y)^2$.

[31] If $r_x = c_x$ and $r_y = c_y$, the two schemes come into close agreement. Then the difference between the two expressions for $4f_{ij}^{n+1}$ can be recognized as the finite difference expression for $r_x r_y (\Delta x)^2 (\Delta y)^2 (\partial^4 f/\partial^2 x \partial^2 y)$. The corresponding difference in $\partial f/\partial t$ is

$$D_{xx} D_{yy} \Delta t \frac{\partial^4 f}{\partial x^2 \partial y^2}. \tag{B4}$$

This extraneous term vanishes as $\Delta t \to 0$.

[32] The conditions $r_x = c_x$ and $r_y = c_y$ are equivalent to $2D_{xx}\Delta t/(\Delta x)^2 = 1$ and $2D_{yy}\Delta t/(\Delta y)^2 = 1$, respectively. Then the combination $2D_{xx}\Delta t/(\Delta x)^2 + 2D_{yy}\Delta t/(\Delta y)^2$ has the value 2, while the CFL stability criterion for the explicit scheme (for the original diffusion equation) requires it to be less than one. Thus for the simple case discussed above, the layer method may be interpreted as an explicit scheme run at an unstably large time step, but stabilized by the small extra term of $\mathcal{O}(\Delta t)$, which is the same order as the error of both methods. This is analogous to grid diffusivity terms added to finite difference schemes in the Lax method.

[33] **Acknowledgments.** This work is supported by NASA grants NNG05GJ95G, NNX08AM36G, and NNX08A155G, by NSF grant ATM-0639772, and by the Space Vehicles Directorate of the Air Force Research Laboratory. This material is based upon work supported in part by CISM, which is funded by the STC Program of the National Science Foundation under agreement ATM-0120950.

[34] Zuyin Pu thanks T. Paul O'Brien and Fuliang Xiao for their assistance in evaluating this paper.

References

Albert, J. M. (2004), Using quasi-linear diffusion to model acceleration and loss from wave-particle interactions, *Space Weather*, *2*, S09S03, doi:10.1029/2004SW000069.

Albert, J. M. (2008), Efficient approximations of quasi-linear diffusion coefficients in the radiation belts, *J. Geophys. Res.*, *113*, A06208, doi:10.1029/2007JA012936.

Albert, J. M., and S. L. Young (2005), Multidimensional quasi-linear diffusion of radiation belt electrons, *Geophys. Res. Lett.*, *32*, L14110, doi:10.1029/2005GL023191.

Baker, D. N., J. B. Blake, R. W. Klebesadel, and P. R. Higbie (1986), Highly relativistic electrons in the Earth's outer magnetosphere: 1. Lifetimes and temporal history 1979–1984, *J. Geophys. Res.*, *91*, 4265–4276.

Baker, D. N., J. B. Blake, L. B. Callis, J. R. Cummings, D. Hovestadt, S. Kanekal, B. Klecker, R. A. Mewaldt, and R. D. Zwickl (1994), Relativistic electron acceleration and decay time scales in the inner and outer radiation belts: SAMPEX, *Geophys. Res. Lett.*, *21*, 409–412.

Baker, D. N., et al. (1997), Recurrent geomagnetic storms and relativistic electron enhancements in the outer magnetosphere: ISTP coordinated measurements, *J. Geophys. Res.*, *102*(A7), 14,141–14,148.

Gardiner, C. W. (1985), *Hondbook of Stochastic Methods for Physics, Chemistry, ond the Naturol Sciences*, Springer-Verlag, Berlin.

Horne, R. B., and R. M. Thorne (1998), Potential waves for relativistic electron scattering and stochastic acceleration during magnetic storms, *Geophys. Res. Lett.*, *25*(15), 3011–3014.

Horne, R. B., and R. M. Thorne (2003), Relativistic electron acceleration and precipitation during resonant interactions with whistler-mode chorus, *Geophys. Res. Lett.*, *30*(10), 1527, doi:10.1029/2003GL016973.

Horne, R. B., S. A. Glauert, and R. M. Thorne (2003), Resonant diffusion of radiation belt electrons by whistler-mode chorus, *Geophys. Res. Lett.*, *30*(9), 1493, doi:10.1029/2003GL016963.

Horne, R. B., R. M. Thorne, S. A. Glauert, J. M. Albert, N. P. Meredith, and R. R. Anderson (2005), Timescale for radiation belt electron acceleration by whistler mode chorus waves, *J. Geophys. Res.*, *110*, A03225, doi:10.1029/2004JA010811.

Horne, R. B., R. M. Thorne, S. A. Glauert, N. P. Meredith, D. Pokhotelov, and O. Santolík (2007), Electron acceleration in the Van Allen radiation belts by fast magnetosonic waves, *Geophys. Res. Lett.*, *34*, L17107, doi:10.1029/2007GL030267.

Li, W., Y. Y. Shprits, and R. M. Thorne (2007), Dynamic evolution of energetic outer zone electrons due to wave-particle interactions during storms, *J. Geophys. Res.*, *112*, A10220, doi:10.1029/2007JA012368.

Lyons, L. R., and R. M. Thorne (1973), Equilibrium structure of radiation belt electrons, *J. Geophys. Res.*, *78*(13), 2142–2149.

Meredith, N. P., R. B. Horne, and R. R. Anderson (2008), Survey of magnetosonic waves and proton ring distributions in the Earth's inner magnetosphere, *J. Geophys. Res.*, *113*, A06213, doi:10.1029/2007JA012975.

Milstein, G. N. (2002), The probability approach to numerical solution of nonlinear parabolic equations, *Numer. Methods for Partial Differentiol Equations*, *18*, 490–522, doi:10.1002/num.10020.

Milstein, G. N., and M. V. Tretyakov (2001), Numerical solution of the Dirichlet problem for nonlinear parabolic equations by a probabilistic approach, *IMA J. Numer. Anal.*, *21*, 887–917.

Milstein, G. N., and M. V. Tretyakov (2002), A probabilistic approach to the solution of the neumann problem for nonlinear parabolic equations, *IMA J. Numer. Anal.*, *22*, 599–622.

Summers, D., and R. M. Thorne (2003), Relativistic electron pitch-angle scattering by electromagnetic ion cyclotron waves during geomagnetic storms, *J. Geophys. Res.*, *108*(A4), 1143, doi:10.1029/2002JA009489.

Tao, X., A. A. Chan, J. M. Albert, and J. A. Miller (2008), Stochastic modeling of multidimensional diffusion in the radiation belts, *J. Geophys. Res.*, *113*, A07212, doi:10.1029/2007JA012985.

Varotsou, A., D. Boscher, S. Bourdarie, R. B. Horne, S. A. Glauert, and N. P. Meredith (2005), Simulation of the outer radiation belt electrons near geosynchronous orbit including both radial diffusion and resonant interaction with whistler-mode chorus waves, *Geophys. Res. Lett.*, *32*, L19106, doi:10.1029/2005GL023282.

Xiao, F., H. He, Q. Zhou, H. Zheng, and S. Wang (2006), Relativistic diffusion coefficients for superluminous (auroral kilometric radiation) wave modes in space plasmas, *J. Geophys. Res.*, *111*, A11201, doi:10.1029/2006JA011865.

Xiao, F., L. Chen, H. Zheng, and S. Wang (2007), A parametric ray tracing study of superluminous auroral kilometric radiation wave modes, *J. Geophys. Res.*, *112*, A10214, doi:10.1029/2006JA012178.

Xiao, F., C. Shen, Y. Wang, H. Zheng, and S. Wang (2008), Energetic electron distributions fitted with a relativistic kappa-type function at geosynchronous orbit, *J. Geophys. Res.*, *113*, A05203, doi:10.1029/2007JA012903.

J. M. Albert, Air Force Research Laboratory, AFRL/RVBX, 29 Randolph Road, Hanscom AFB, MA 01731-3010, USA.

A. A. Chan and X. Tao, Department of Physics and Astronomy, Rice University, MS 108, 6100 Main Street, Houston, TX 77005-1892, USA. (aac@rice.edu; xtao@rice.edu)